

# Multivariable output feedback stabilisation with structure constraint: application to a gyrometer

Benoit Boivin and Laurent Rambault and Patrick Coirault and Claude Dewez

**Abstract**—In this paper, the problem of static output feedback control of a linear system is considered. This method allows to design a PID controller in order to taking into account the industrial context. The proposed algorithm is used to perform a multivariable PID controller applied to design a sensor. The system, a gyrometer, is an angular velocity sensor used as instrument of navigation for aeronautics. The numerical results presented are obtained from real system and real time board.

## I. INTRODUCTION

This paper presents the study of the mathematical model of a vibrating gyrometer and its control using a multivariable PID controller. The PID controller structure is prescribed by the industrial context. Before the work developed in this paper, a continuous time controller has been designed and has been implemented in the industrial laboratory. The method used to design the controller is an experimental one. The main interest of this paper is to propose an effective method to design a PID controller for a MIMO industrial system. To perform the controller, the problem of static output feedback is considered and modified to introduce the structure constraint [4]. The main objective is to stabilise the gyrometer with a multivariable PID controller in order to improve the robustness when physical modifications are introduced.

The gyrometer is an angular velocity sensor used for the design of the instruments of navigation for aeronautics. Its principle is based on the detection of Coriolis accelerations introduced by the mechanical vibrations. This sensor brings into mechanical phenomena (vibrations of a resonator) and electromagnetic (excitation and detection of these vibrations). The objective of the controller applied to this system is to guarantee the linearity of the sensor. The output signal must be represented as follow:

$$i_s = K_1 (\Omega + K_0),$$

with constants  $K_0$  and  $K_1$ .  $K_1$  represents the scale factor,  $K_0$  the bias and  $\Omega$  the real rotate speed to measure. The difficulty lies in the fact that, on the one hand, the various

This work is funded by Thales Avionics. The authors gratefully acknowledge the support of this research by Thales Avionics through provision of a research team

Benoit Boivin is with LAII, University of Poitiers, France  
Benoit.Boivin@univ-poitiers.fr

Laurent Rambault is with LAII, University of Poitiers, France  
Laurent.Rambault@univ-poitiers.fr

Patrick Coirault is with LAII, University of Poitiers, France  
Patrick.Coirault@univ-poitiers.fr

Claude Dewez is with LAII, University of Poitiers, France  
claude.dewez@univ-poitiers.fr

electric signals are oscillating and on the other hand, the control signals and the signals of measurements are multiplexed. They can't coexist simultaneously. A continuous time controller has been tested by the company Thales Avionics.

The second section presents the algorithm used to design the PID. The third section presents the physical principle of the gyrometer and its model used for the multivariable PID controller design. The fourth section concerns numerical results.

## II. MULTIVARIABLE OUTPUT FEEDBACK STABILISATION

Proportional Integral Derivative controllers are still widely used in industrial processes. Its popularity is due to its simplicity and needs only three parameters to tune. However, the three PID parameters should be tune appropriately in order to satisfy control performance.

The problem of design a multivariable PID controller is formulated in a LMI framework [1].

Concerning the application proposed in this paper, the PID controller is designed with experimental approach. The objective is to achieve a better performance of the control than the initial controller.

The method used in this paper concerns the feedback stabilization. In this section, we just summarize the technique. For more details the reader is invited to see [5].

The first step is to transform the PID controller to static output feedback.

Consider the linear time invariant system:

$$\dot{x} = Ax + Bu, y = Cx \quad (1)$$

and the following PID controller

$$u = F_1 y + F_2 \int_0^t y(\alpha) d(\alpha) + F_3 \frac{dy}{dt} \quad (2)$$

where  $x(t) \in R^n$  represents the state vector,  $u(t) \in R^l$  represents the control vector and  $y(t) \in R^m$  represents the output vector.

$F_1, F_2, F_3$  are matrices to be designed. The controller obtained is an ideal PID controller and need some modifications to be implemented into a real time board.

Lets consider  $z = [z_1^T z_2^T]^T$  the new state space vector where:  $z_1 = x$  and  $z_2 = \int_0^t y(\alpha) d(\alpha)$ .

The state space equation of the new system can be written as:

$$\begin{aligned} \dot{z} &= \bar{A}z + \bar{B}u, \\ \bar{y}_i &= \bar{C}_i z, i = 1, 2, 3 \end{aligned} \quad (3)$$

where

$$\bar{A} = \begin{bmatrix} A & 0 \\ C & 0 \end{bmatrix}, \bar{B} = \begin{bmatrix} B \\ 0 \end{bmatrix}$$

$$\bar{C}_1 = [C0], \bar{C}_2 = [0I]\bar{C}_3 = [CA0]$$

Our aim is to compute a static output feedback law  $u = \bar{F}\bar{y}$  that ensures the stability of the closed-loop system  $\bar{A}_{cl} = \bar{A} + \bar{B}\bar{F}\bar{C}$ .

The control law can be rewritten as:

$$u = F_1\bar{y}_1 + F_2\bar{y}_2 + F_3\bar{y}_3 + F_3CBu.$$

Suppose the matrix  $(I - F_3CB)$  is invertible.

$$\bar{y} = [\bar{y}_1^T \bar{y}_2^T \bar{y}_3^T]^T,$$

$$\bar{C} = [\bar{C}_1^T \bar{C}_2^T \bar{C}_3^T]^T,$$

$$\bar{F} = [\bar{F}_1 \bar{F}_2 \bar{F}_3],$$

$$\bar{F} = [(I - F_3CB)^{-1}F_1(I - F_3CB)^{-1}F_2(I - F_3CB)^{-1}F_3].$$

So the problem of PID controller design reduces so that of static output feedback controller design apply of the following system:

$$\dot{z} = \bar{A}z + \bar{B}u, \bar{y} = \bar{C}z, u = \bar{F}\bar{y}.$$

Before stating the problem, we recall the following lemma [2].

**Lemma 1**

*System (1) is stabilizable via static output feedback if and only if there exist matrices  $P > 0$  and  $F$  satisfying the following matrix inequality:*

$$\begin{aligned} A^T P + PA - PBB^T P + \\ (B^T P + FC)^T (B^T P + FC) < 0 \end{aligned} \quad (5)$$

The term  $-PBB^T P$  increases the difficulty to find a solution. A possible way to propose an efficient tool by using the LMI tools is described in [2].

The solution is described by the following LMI algorithm [5].

**Initial data:** System's state space realization  $(\bar{A}, \bar{B}, \bar{C})$ .

**Step 1:** Choose  $Q_0 > 0$  and solve  $P$  for the Riccati equation:  $\bar{A}^T P + P\bar{A} - P\bar{B}\bar{B}^T P + Q_0 = 0, P > 0$ .

Set  $i = 1$  and  $X_1 = P$ .

**Step 2:** Solve the following optimization problem for  $P_i, \bar{F}$  and  $\alpha_i$ : Minimize  $\alpha_i$  subject to the constraint LMIs:

$$\begin{bmatrix} \Sigma_{1i} & (\bar{B}^T P_i + \bar{F}\bar{C})^T \\ \bar{B}^T P_i + \bar{F}\bar{C} & -I \end{bmatrix} < 0, P_i > 0$$

$$I + (\bar{C}\bar{B}\bar{F}_3)^T + \bar{C}\bar{B}\bar{F}_3 > 0$$

where  $\Sigma_{1i} = \bar{A}^T P_i + P_i \bar{A} - X_i \bar{B} \bar{B}^T P_i - P_i \bar{B} \bar{B}^T X_i + X_i \bar{B} \bar{B}^T X_i - \alpha_i P_i$ . Denote by  $\alpha_i^*$  the minimized value of  $\alpha_i$ .

**Step 3:** If  $\alpha_i^* \leq 0$ , the matrix pair  $(P_i, \bar{F})$  solves static output feedback problem. Stop. Otherwise go to Step 4.

**Step 4:** Solve the optimization problem for  $P_i$  and  $\bar{F}$ : Minimize  $tr(P_i)$  subject to the constraint following LMIs with  $\alpha_i = \alpha_i^*$  ( $tr$  stands for the trace of a square matrix):

$$\begin{bmatrix} \Sigma_{1i} & (\bar{B}^T P_i + \bar{F}\bar{C})^T \\ \bar{B}^T P_i + \bar{F}\bar{C} & -I \end{bmatrix} < 0, P_i > 0$$

$$I + (\bar{C}\bar{B}\bar{F}_3)^T + \bar{C}\bar{B}\bar{F}_3 > 0$$

where  $\Sigma_{1i} = \bar{A}^T P_i + P_i \bar{A} - X_i \bar{B} \bar{B}^T P_i - P_i \bar{B} \bar{B}^T X_i + X_i \bar{B} \bar{B}^T X_i - \alpha_i P_i$ .

Denote by  $P_i^*$  the optimal value of  $P_i$ .

**Step 5:** If  $\|X_i \bar{B} - P_i^* \bar{B}\| < \varepsilon$ , where  $\varepsilon$  is a prescribes tolerance, go to Step 6; otherwise set  $i = i + 1, X_i = P_i^*$ , and go to Step 2.

**Step 6:** It cannot be decided by this algorithm whether static output feedback problem is solvable. Stop.

The properties of solution series  $\alpha_i^*$  and  $P_i^*$  are given in [2].

### III. APPLICATION TO A GYROMETER

#### A. Physical Description

There exists many technics to perform gyroscope. One of them is based on the Coriolis effect in order to measure an angular velocity. The gyroscope consists of an elastic body such that one of its resonant modes is excited to constant amplitude vibrations (drive mode). Inducing rate about a particular body-fixed axis excites a different resonant mode into vibration (output mode). Generally, the rate by which the energy transfers from the first to the second mode is a measure of the induced rate. In an open-loop mode, the amplitude of the second mode is a measure to the rate, while in a closed-loop mode the rebalancing force allows the measure. For this application, the vibrating gyroscope employs inductance sensing for the second mode vibrations.

Fig. 1 shows the structure of the gyroscope. It is composed of an elastic hollow cylinder, and a set of coils distributed around the cylinder. A permanent magnetic field is induced by a d.c. current exciting the polarization coils.

By applying an alternating current to the excitation coils, a first mechanical mode of the elastic cylinder is excited into vibrations Fig. 2.

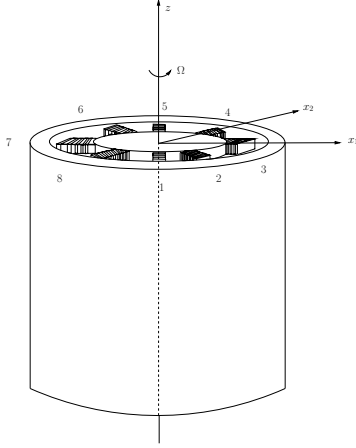


Fig. 1. Gyroscope structure: polarization coils (1 to 8) excitation coils (1,3,5,7), rebalancing coils (2,4,6,8)

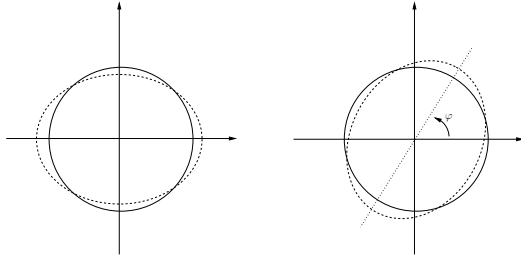


Fig. 2. Oscillatory motion of mass

The oscillation of the cylinder is an elliptical motion, that vibrates at the frequency of the magnetic field. If the cylinder is subjected to revolutions around z-axis with an angular rate  $\Omega(t)$ , the elliptical motion is driven with the cylinder, with an opposite and lower speed  $\varphi(t) = -\frac{k_c}{2}\Omega(t)$ , where  $k_c$  depends on the gyroscope geometry (see Fig. 3).

$X(\theta, t) = x_0(t) \cos(2(\theta - \varphi))$  is the displacement of the cylinder in the radial direction. Projecting  $X(\theta, t)$  on the body-fixed axis  $x_1$  and  $x_2$  gives (see Fig. 4)

$$X(\theta, t) = x_1(t) \cos(2\theta) + x_2(t) \sin(2\theta)$$

with

$$\begin{aligned} x_1(t) &= x_0(t) \cos(2\varphi(t)) \\ x_2(t) &= x_0(t) \sin(2\varphi(t)) \end{aligned}$$

$x_1(t)$  and  $x_2(t)$  represent the magnitudes of the resulting oscillatory motion in two fixed points belonging to the cylinder. They induce electromagnetic currents in coils. To maintain constant the elliptical motion (i.e.  $\varphi(t) = 0$ ) needs to generate a second vibratory mode along  $x_1$  and  $x_2$  axes (fig. 5). In closed-loop mode, the electromagnetic counterbalancing forces  $F_1$  and  $F_2$  are such that  $x_2(t) = 0$ .

### B. Mathematical Model

The state space representation is given by (6)

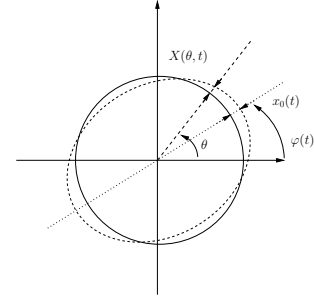


Fig. 3. Elliptical motion during rotation

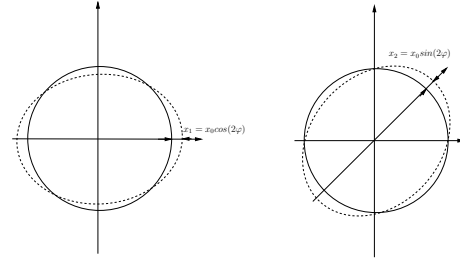


Fig. 4. Projection of the elliptical motion

$$\left\{ \begin{aligned} \begin{bmatrix} \ddot{x}_1 \\ \dot{x}_1 \\ \ddot{x}_2 \\ \dot{x}_2 \end{bmatrix} &= \begin{bmatrix} -\frac{A}{M} & -\frac{K}{M} & \frac{2Mc\Omega}{M} & 0 \\ 1 & 0 & 0 & 0 \\ -\frac{2Mc\Omega}{M} & 0 & -\frac{A}{M} & -\frac{K}{M} \\ 0 & 0 & 1 & 0 \end{bmatrix} \begin{bmatrix} x_1 \\ x_2 \\ \dot{x}_1 \\ \dot{x}_2 \end{bmatrix} \\ &+ \begin{bmatrix} \frac{G_{exc}K_z^2}{M} & 0 \\ 0 & 0 \\ 0 & \frac{G_{exc}K_z^2}{M} \\ 0 & 0 \end{bmatrix} \begin{bmatrix} i_1 \\ i_2 \end{bmatrix} \\ \begin{bmatrix} u_1 \\ u_2 \end{bmatrix} &= \begin{bmatrix} G_{det} & 0 & 0 & 0 \\ 0 & 0 & G_{det} & 0 \end{bmatrix} \begin{bmatrix} \dot{x}_1 \\ x_1 \\ \dot{x}_2 \\ x_2 \end{bmatrix} \end{aligned} \right.$$

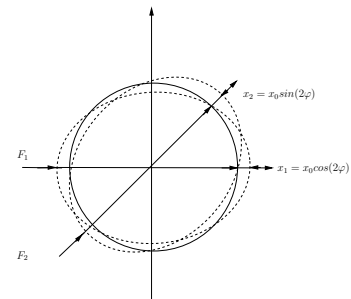


Fig. 5. Counterbalancing forces  $F_1$  and  $F_2$

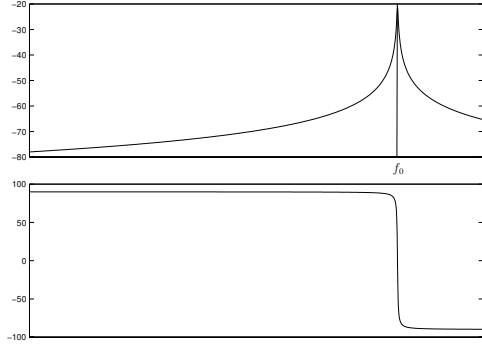


Fig. 6. Bode plot for a subsystem

where

- $M$  mass of cylinder,
- $K$  coefficient for the stiffness,
- $A$  Damping ratio,
- $M_c$  mass of Coriolis,
- $K_z$  coefficient that depends on longitudinal position of plan of excitation/detection,
- $G_{exc}$  gain for the excitation,
- $G_{det}$  gain for the detection.

The model defined above has two inputs and two outputs. Furthermore, it is nonlinear and from the rotate speed, a coupling between the axes 1 and 2 appeared.

$$U_1(p) = \frac{G_{det}G_{exc}K_z^2p}{Mp^2 + Ap + K}I_1(p) + \frac{2M_c\Omega p}{Mp^2 + Ap + K}U_2(p)$$

and

$$U_2(p) = \frac{G_{det}G_{exc}K_z^2p}{Mp^2 + Ap + K}I_2(p) - \frac{2M_c\Omega p}{Mp^2 + Ap + K}U_1(p)$$

The Bode plot for functions  $H_i(p) = \frac{U_i(p)}{I_i(p)}$  is given on Fig. 6.

$f_0$  represents the frequency of resonance for the considered system. The properties which are considered take place around this frequency. To highlight those properties and to be able to control the system around  $f_0$ , we purpose to shift the model in low frequency. To do this, we use the complex signal with the help of Hilbert transform.

The various signals in the system can be written as:

$$x = X \cos(\omega_0 t + \Phi) \quad (6)$$

It is possible to introduce the analytical signal described by (7).

$$x = \underline{X}e^{j\omega_0 t} \quad (7)$$

where  $\underline{X} = Xe^{j\Phi}$  represents the complex envelope of the signal.

By simplifying by  $e^{j\omega_0}$  and separating the imaginary part and the real part, we obtain the state space following representation.

$$\dot{X} = A.X + B.I, U = C.X \quad (8)$$

with

$$X = \begin{bmatrix} \dot{X}_{1Re} & X_{1Re} & \dot{X}_{1Im} & \dot{X}_{2Re} & X_{2Re} & X_{1Im} \\ \dot{X}_{2Im} & X_{2Im} \end{bmatrix}^T$$

$$I = \begin{bmatrix} I_{1Re} & I_{1Im} & I_{2Re} & I_{2Im} \end{bmatrix}^T$$

$$U = \begin{bmatrix} U_{1Re} & U_{1Im} & U_{2Re} & U_{2Im} \end{bmatrix}^T$$

$$A = \begin{bmatrix} -\frac{A}{M} & \omega_0^2 - \frac{K}{M} & 2\omega_0 & \frac{\omega_0 A}{M} & \dots \\ 1 & 0 & 0 & 0 & \dots \\ -2\omega_0 & -\frac{\omega_0 A}{M} & -\frac{A}{M} & \omega_0^2 - \frac{K}{M} & \dots \\ 0 & 0 & 1 & 0 & \dots \\ -\frac{2M_c\Omega}{M} & 0 & 0 & \frac{2\omega_0 M_c\Omega}{M} & \dots \\ 0 & 0 & 0 & 0 & \dots \\ 0 & -\frac{2\omega_0 M_c\Omega}{M} & -\frac{2M_c\Omega}{M} & 0 & \dots \\ 0 & 0 & 0 & 0 & \dots \\ \frac{2M_c\Omega}{M} & 0 & 0 & -\frac{2\omega_0 M_c\Omega}{M} & \dots \\ 0 & 0 & 0 & 0 & \dots \\ 0 & \frac{2\omega_0 M_c\Omega}{M} & \frac{2M_c\Omega}{M} & 0 & \dots \\ 0 & 0 & 0 & 0 & \dots \\ -\frac{A}{M} & \omega_0^2 - \frac{K}{M} & 2\omega_0 & \frac{\omega_0 A}{M} & \dots \\ 1 & 0 & 0 & 0 & \dots \\ -2\omega_0 & -\frac{\omega_0 A}{M} & -\frac{A}{M} & \omega_0^2 - \frac{K}{M} & \dots \\ 0 & 0 & 1 & 0 & \dots \end{bmatrix}$$

$$B = \begin{bmatrix} \frac{G_{exc}K_z^2}{M} & 0 & 0 & 0 \\ 0 & 0 & 0 & 0 \\ 0 & \frac{G_{exc}K_z^2}{M} & 0 & 0 \\ 0 & 0 & 0 & 0 \\ 0 & 0 & \frac{G_{exc}K_z^2}{M} & 0 \\ 0 & 0 & 0 & 0 \\ 0 & 0 & 0 & \frac{G_{exc}K_z^2}{M} \\ 0 & 0 & 0 & 0 \end{bmatrix}$$

$$C = \begin{bmatrix} G_{det} & 0 & 0 & 0 \\ 0 & w_0 G_{det} & 0 & 0 \\ 0 & G_{det} & 0 & 0 \\ -w_0 G_{det} & 0 & 0 & 0 \\ 0 & 0 & G_{det} & 0 \\ 0 & 0 & 0 & w_0 G_{det} \\ 0 & 0 & 0 & G_{det} \\ 0 & 0 & -w_0 G_{det} & 0 \end{bmatrix}^T$$

This low frequency mathematical model has been used to perform the PID controller.

#### IV. EXPERIMENTAL RESULTS

The methodology developed in section 2 with the help of LMI Tool box [3] is applied to the model given in the previous section. The objective is to perform a multivariable PID controller to achieve the stability of the system. The controller is defined by matrices  $F_1$  (proportional effect),  $F_2$  (integral effect) and  $F_3$  (derivative effect).

$$F1 = \begin{bmatrix} 5.0320 & 6.4070 & -0.4414 & -0.0622 \\ -6.4071 & 5.0320 & 0.0622 & -0.4414 \\ 0.4375 & 0.0647 & 5.0334 & 6.4059 \\ -0.0648 & 0.4375 & -6.4059 & 5.0334 \end{bmatrix}$$

$$F2 = 10^{-5} \begin{bmatrix} -0.3545 & 0.0294 & -0.0036 & -0.0046 \\ -0.0262 & -0.3515 & 0.0016 & -0.0005 \\ 0.0005 & 0.0015 & -0.3514 & 0.0263 \\ -0.0045 & 0.0036 & -0.0294 & -0.3545 \end{bmatrix}$$

$$F3 = \begin{bmatrix} 0.9414 & 0.0756 & -0.0041 & -0.0004 \\ -0.0756 & 0.9414 & 0.0004 & -0.0041 \\ 0.0041 & 0.0009 & 0.9414 & 0.0755 \\ -0.0009 & 0.0041 & -0.0755 & 0.9414 \end{bmatrix}$$

The plots given in Fig.7, Fig.8, Fig.9 and Fig.10 have been obtained with the real system.

The Fig.7 shows the linearity domain in open loop and closed-loop configuration.

The frequency response is given in Fig.8.

The step responses of the sensor appear in Fig.9 and Fig.10.

#### V. CONCLUSION

##### A. Conclusions

This paper develops a methodology to design PID controller in order to taking into account the industrial con-

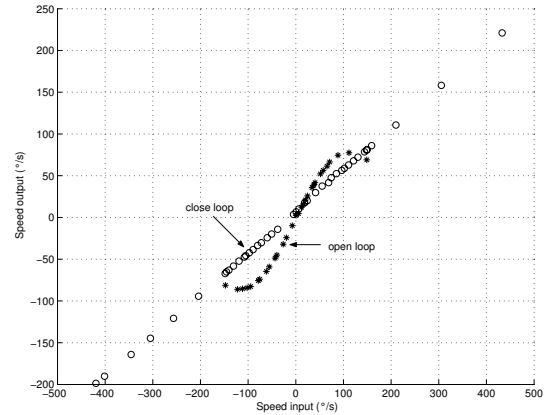


Fig. 7. Static transfer for open-loop and closed-loop

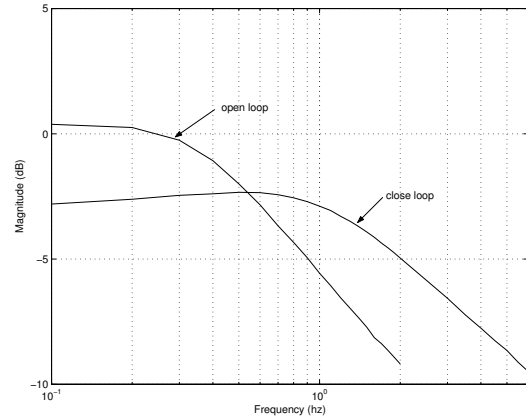


Fig. 8. Bode response for open-loop and closed-loop

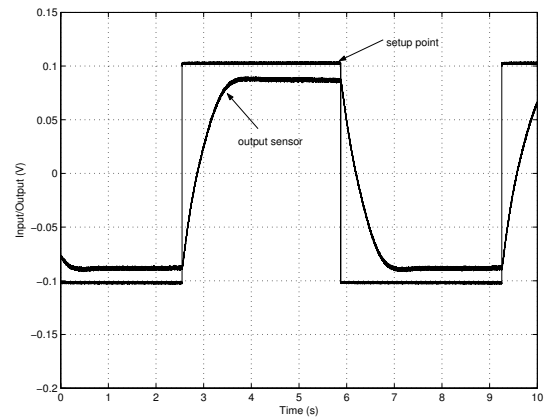


Fig. 9. Step response for open-loop system

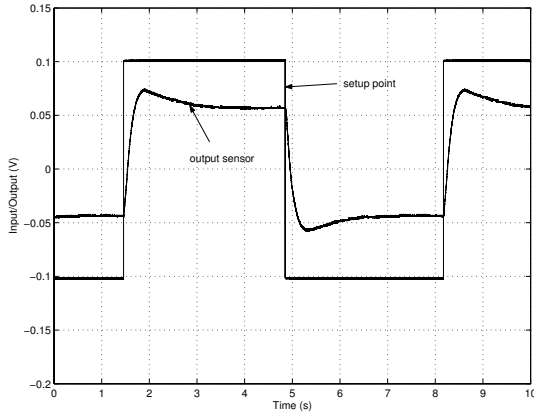


Fig. 10. Step response for closed-loop system

straint. The contribution of this paper is to design a sensor applied to the aeronautic system with the help of control theory. The two main problems are the multiplexing to avoid the magnetic coupling and the high quality factor of the cylinder. To overcome these problems, we establish the model of the system in low frequency by using the Hilbert transform.

An efficient algorithm based on LMI technique is proposed to solve the problem of multivariable PID controller in an industrial context. The controller presented in the previous section has been implemented with success in a real time board. The multivariable PID is implemented in a FPGA component.

#### B. Future Works

The perspectives of this work concern the analysis of robustness of the stability. In fact some physical "defaults" modify the magnetic behaviour of the system by introducing coupling and non linearity. Two point of view are considered: the first one is an experimental analysis of robustness and the second one is the mathematical analysis.

#### REFERENCES

- [1] S. Boyd and L. El Ghaoui and E. Feron and V. Balakrishnan, *Linear Matrix Inequalities in System and Control Theory*, SIAM, Philadelphia, 1994.
- [2] Y.Y. Cao and J. Lam and Y.X. Sun, Static output feedback stabilization: An ILMI approach, *Automatica*, vol. 34, 1998, pp 1641-1645.
- [3] P. Gahinet and A. Nemirovski and J. Laub and M. Chilali, *LMI Control Toolbox*, The Math Works Inc, 1995.
- [4] V.L. Syrmos and C.T. Abdallah and P. Dorato and K. Grigoriadis, Static output feedback - a survey, *Automatica*, vol. 33, 1997, pp 125-137.
- [5] F. Zheng and Q.G. Wang and T.H. Lee, On the design of multivariable PID controllers via LMI approach, *Automatica*, vol. 38, 2002, pp 265-271.